MEMS-based IMU Assisted Real Time Difference Using Raw Measurements for Smartphone

Zida Wu, Peilin Liu, Qiang Liu, Yuze Wang
Shanghai Jiao Tong University, China

BIOGRAPHIES

Zida Wu is a master student in the Department of Electronic Engineering at Shanghai Jiao Tong University. He received the B.S. degree from Xidian University, Xi'an, China. His main research is in the areas of low-cost GNSS difference positioning.
Peilin Liu is a professor of the Department of Electronic Engineering at Shanghai Jiao Tong University. She received her Ph.D. from the University of Tokyo, Tokyo, Japan. Her main research is in the areas of GNSS System-on-Chip architecture design and communication signal processing.
Qiang Liu received the B.S. degree from East China Normal University, Shanghai, China, in 2015. He is currently working toward the Doctor's degree in Shanghai Jiao Tong University, Shanghai, China. His research interests include high precision GNSS positioning with low power device and integrated GNSS/MEMS-based INS navigation.
Yuze Wang is a Ph.D. student in Shanghai Jiao Tong University, Shanghai, China. He received the M.S. degree from Harbin Institute of Technology, Harbin, China. His research topic is GNSS signal characteristics modeling and multipath mitigation technology etc.

ABSTRACT

Google released Android Nougat (version 7.0) in 2016, which opens the possibility to use raw data to achieve high precision solutions on low-cost smart devices. Due to the poor performance of the low-cost antenna and crystal oscillator of smartphone, the accuracy of traditional single point positioning can only reach about 10 meters. The target of this paper is to propose a pseudorange double difference (PDD) with IMU assisted model on smartphone. Real-time difference assisted by IMU positioning algorithm was first applied to realize high-precision positioning on stand-long smartphone platform. Three groups of pedestrian scenes positioning comparison experiments were carried out. The results show that MEMS-based IMU assisted PDD increases smartphone positioning precision and robustness, and the horizonal mean error can be less than 4 meters. It demonstrated that the algorithm can effectively stabilize the performance of smartphone positioning. The significance of this work is to prove that RTD assisted by IMU on low-cost mobile platform is feasible and this algorithm exhibits better performance than traditional positioning solutions.

I. INTRODUCTION

In the last decades, positioning accuracy of GNSS navigation has been greatly improved, and the performance of low-cost equipment cannot meet the market demand compared with survey-grade equipment. Many particular positioning applications are faced to the ubiquitously available smartphone such as offline shopping or open-air parking. For meter-grade precision positioning, the widely application is to make use of Wi-Fi signals with predetermined database [1] or multi-antennas positioning based on angle-of-arrival (AoA) techniques [11], [12], but the ideal solution is employing smartphone original GNSS data and internal sensors for high-accuracy positioning, such as inertial measurement unit (IMU).

Code derived pseudorange and carrier-phase are the particularly useful observables for GNSS positioning. Prior work [2] has shown that effective time of carrier-phase continuous tracking time was less than 5 minutes on smartphone, after that PLL would go into duty-cycling model to reduce power consumption. Easy lock and frequent cycle slip also constrain this application. Pseudorange is the only adequate way to be considered. Research showed [3] that the main obstacles of high-accuracy positioning of low-cost navigation come from the poor antenna multipath suppression and irregular gain pattern result in large time-correlated phase error, internal thermal noise and clock errors also play a significant role. However, a main drawback of IMU in smartphone is that the unit owes high instability and oscillation noise which would lead to terrible sensor errors.

Pesyna[3] and TE Humphreys[4] demonstrated that smartphone antenna and GNSS chips enable to achieve high-accuracy positioning. However, they only used smartphone antenna and chips separately to connect to an external receiver because the raw GNSS data was unavailable, where professional receiver enjoyed the better sensitivity and multipath suppression to generate observations. In May 2016, Google announced that smartphone can retrieve raw GNSS measurements via the corresponding programming interface (API) with Android Nougat (version 7) operating system or later [5]. Then Google released the GnssLogger application to acquire the raw data with its source code. With proper method the raw data could be parsed into a standard RINEX format observation file. Richard Langley [2] examined the quality of the data with the purpose of deriving precise positioning information from a smartphone, the report confirmed that noisy pseudorange observations enable provide meter-level accuracies. The limitation of the result is that the work focused on migrating related error so all data was post-processed and they replaced the broadcast ephemeris by other precise satellite orbit and clock corrections. Wonho Kang [6] demonstrated that MEMS-based IMU enable to provide efficient navi-information by means of appropriate combination way.

This paper preliminary made three main contributions. First, we tested and verified the feasibility of precise positioning on a stand- alone smartphone platform using raw GNSS data. The problems encountered during the process were also presented in this paper. Second, RTD was first applied on smartphone and this paper offered an analysis of the advantages to traditional single point positioning. Third, it demonstrated that the scheme that MEMS-based IMU assisted PDD navigation is feasible, even the low-cost IMU inside smartphone instability is unstable.

In this paper, section II first introduces the PDD positioning model and clarifies the advantages to traditional method. Section III describes the data collection and process, simultaneously points out the problem we met. Section IV presents the results of system performance. A brief conclusion is finally given. Our system was tested on HUAWEI P10, all results were compared with U-blox-m8n with South HY-BLRB02R antenna.

II. PDD MODEL AND IMU INTEGRATION SCHEME

Kalman filter was induced in the algorithm. Pseudorange and Doppler observation equations are as follows:

$$\begin{aligned} \rho_u^{(n)} &= r_u^{(n)} + \delta t_u - \delta t^{(n)} + \chi_u^n + T_u^n + \xi_{\rho u}^{(n)} \\ \dot{\rho}_u^{(n)} &- v^{(n)} \cdot I_u + \delta f^{(n)} - \xi_{\rho u}^{(n)} = -v_u \cdot I_u + \delta f_u \end{aligned} \tag{1}$$

where $\boldsymbol{\rho}$ is the pseudorange derived from time difference between transmit time and receive time. $\boldsymbol{r}$ represents the real distance between satellite and user. $\boldsymbol{\chi}$ and $\boldsymbol{T}$ means the ionosphere and troposphere error, $\boldsymbol{\xi}$ describes the other errors for the pseudorange measure and $\boldsymbol{f}$ describes the frequency drift in the function. $\boldsymbol{I}$ means the direction vector of user to satellite. $\boldsymbol{v}$ represents the velocity of user or satellite, all the superscripts denote satellites and the subscripts denote receivers state.

Traditional Kalman filter (KF) was only for linear control system, direct single point positioning is no longer a linear process as equation above. Extend Kalman filter (EKF) should be induced to apply this estimation. Moreover, Ionosphere and troposphere generally result dozens of meters errors. The rover baseline direction vector $\boldsymbol{I_r}$ stability is unreliable especially the $\boldsymbol{I_r}$ was generated by smartphone, it means the position is in coupled relationship with velocity.

Based on short baseline hypothesis, the baseline direction vector of rover and base-station can be regard as parallel lines, $\boldsymbol{I_r = I_u}$. Ionosphere and Troposphere were ignored in short base-line which is less than 10km [8]. Further, $\boldsymbol{r_{ur}}$ can be equal to $\boldsymbol{-b_{ur} \cdot I_r}$. This step avoids to linearize the estimation, EKF is no more needed, and the position is decoupled with velocity because the direction vector $\boldsymbol{I_u}$ is no more determined by user.

Smartphone clock error is an unstable factor, the quality of clock will subsequently analysis in next chapter. Therefore, we adopted double difference to eliminate smartphone clock error. For exchange, PDD will sacrifice one equation in observation, 5 visible satellite is essential.

The short time reliability of IMU denotes that it is an ideal complementary to GNSS system, IMU can continously provide high update rate data while GNSS update rate is only 1HZ. Meanwhile IMU information do not depend on external signal so when signal blockage the IMU information is still work. There are two mainstream IMU/GNSS integration schemes for Kalman filter: direct integration and indirect integration. Indirect scheme regards error values as state estimator, it established several state error models to transfer estimator to KF and the KF output would feed back to sub-system. The error state is linear so traditional KF is satisfied. Direct scheme input is IMU or INS (inertail navigation system) data and GNSS variables, and KF result is the system optimal estimate. The original range state estimator is nonliear thus EKF is promoted to establish the linearized equations.

An important difference is that indirect scheme requires two independent sub-navigation-system while direct scheme have no such the strict requirments. On the other hand, the systematic error of MEMS-IMU of smartphone is unkown so the error model is incompele, and terrible performance of smartphone-IMU would lead the cumulative drift losing control. As above analysis, we choose direct integration as the assisted scheme.

Consumer-grade MEMS-based IMU always suffered from system instability and oscillation noise, system instability refers to no accurate scaling, sensor axis misalignment and cross-axis sensitivities [9]. A direct time-domain-analysis technique of IMU noise is Allan variance Model which pointed out the representation of IMU noise terms: quantization noise, angle(velocity) random walk, bias instability, rate random walk and drift rate ramp [10]. By integrating the IMU in the fusion algorithm, these errors will be accumulated, leading to a significant drift in the positioning result. According to experience, the zero bias is the main factor should be considered for accelerometer. The zero bias instability is hard to evaluate, because it is changeable every time. But the zero bias of accelerometer would be fixed down after every time the IMU was power-on. Thus, we let it stand still for a certain time to calculate the bias before positioning, one minute is enough if we only need zero bias.

Therefore, the PDD KF prediction equations as:

$$\begin{bmatrix} b_{ur} \\ v \\ a \\ \delta a \end{bmatrix} = \begin{bmatrix} 1 & T_S & \frac{T_S^2}{2} & 0 \\ 0 & 1 & T_S & 0 \\ 0 & 0 & 1 & 0 \\ 0 & 0 & 0 & 1 \end{bmatrix} \begin{bmatrix} b_{ur} \\ v \\ a \\ \delta a \end{bmatrix} \tag{2}$$

$$P_k = AP_{k-1}A^T + Q_p$$

where

$$\mathbf{Q_p} = \begin{bmatrix} S_x T_S + S_v \frac{T_S^3}{3} + S_a \frac{T_S^5}{20} & S_v \frac{T_S^2}{2} + S_a \frac{T_S^4}{8} & S_a \frac{T_S^3}{6} & 0 \\ S_v \frac{T_S^2}{2} + S_a \frac{T_S^4}{8} & S_v T_S + S_a \frac{T_S^3}{3} & S_a \frac{T_S^2}{2} & 0 \\ S_v \frac{T_S^3}{6} & S_v \frac{T_S^2}{2} & S_a T_S & 0 \\ 0 & 0 & 0 & Q_a \end{bmatrix} \tag{3}$$

where $\boldsymbol{b_{ur}}$ means the base-line vector between user to base-station, $\boldsymbol{v}$ and $\boldsymbol{a}$ respectively represent the velocity and acceleration of user. $\boldsymbol{\delta a}$ means the zero bias of accelerometer. $\boldsymbol{A}$ represents the state transfer matrix form k-1 epoch to k epoch. $\boldsymbol{P}$ and $\boldsymbol{Q}$ respectively represent the root square error matrix and state transfer noise matrix.

Observation equations:

$$\begin{bmatrix} \rho_{ur}^1 - \rho_{ur}^j \\ \rho_{ur}^2 - \rho_{ur}^j \\ \cdots \\ \rho_{ur}^i - \rho_{ur}^j \end{bmatrix} = \begin{bmatrix} -\left[I_r^{(1)} - I_r^{(j)} \right] \cdot v_u \\ -\left[I_r^{(2)} - I_r^{(j)} \right] \cdot v_u \\ \cdots \\ -\left[I_r^{(i)} - I_r^{(j)} \right] \cdot v_u \end{bmatrix}$$

$$\begin{bmatrix} \rho_{ur}^1 - \rho_{ur}^j \\ \rho_{ur}^2 - \rho_{ur}^j \\ \cdots \\ \rho_{ur}^i - \rho_{ur}^j \end{bmatrix} = \begin{bmatrix} -\left[I_r^{(1)} - I_r^{(j)} \right] \cdot b_{ur} \\ -\left[I_r^{(2)} - I_r^{(j)} \right] \cdot b_{ur} \\ \cdots \\ -\left[I_r^{(i)} - I_r^{(j)} \right] \cdot b_{ur} \end{bmatrix} \tag{4}$$

$$K = P_k C^T (C P_k C^T + R)^{-1}$$

where

$$\mathbf{C}=\begin{bmatrix} H_x & 0 & 0 & H_y & 0 & 0 & H_z & 0 & 0 \\ 0 & H_x & 0 & 0 & H_y & 0 & 0 & H_z & 0 \\ 0 & 0 & H_x & 0 & 0 & H_y & 0 & 0 & H_z \\ 0 & 0 & 1 & 1 & 0 & 0 & 0 & 0 & 0 \\ 0 & 0 & 0 & 0 & 1 & 1 & 0 & 0 & 0 \\ 0 & 0 & 0 & 0 & 0 & 0 & 0 & 1 & 1 \end{bmatrix} \tag{5}$$

$$\begin{bmatrix} R_{sat} \\ R_a \end{bmatrix}=\begin{bmatrix} M^2 \times 10^{-CNR^{(i)}/10} \\ R_{ax} \\ R_{ay} \\ R_{az} \end{bmatrix}$$

where $\boldsymbol{\rho_{ur}}$ denotes the user pseudorange value minus base-station pseudorange value. $\boldsymbol{K}$ means gain matrix, $\boldsymbol{R}$ means the observation noise matrix and $\boldsymbol{M}$ is a constant. $\boldsymbol{C}$ means the relationship matrix between observation vector and state vector in KF and $\boldsymbol{H}=\boldsymbol{I_r}^i-\boldsymbol{I_r}^j$ in matrix $\boldsymbol{C}$.

The KF filtering initial value was obtained by least-square (LS) estimation. Although the initial value has little effect as the time of KF iterations increases, the appropriate and correct initial value is conducive to fast convergence. As all equation variables were linear in difference LS model, a large observations error in LS matrix may produce destructive result. An empirically elevation cut-off angle was set to 15 degree.

A precise observation should have higher weight and more reliability than other imprecise ones. Thus, weighted least squares (WLS) was adopted. According to Gerdoan [7] paper, schemes of CNR-based weighted and Elevation-based weighted or combination weighted are no significant differences, so we chose CNR-based weight scheme to reduce amount of calculation. Residual-based RAIM to perform consistency checks was induced to strengthen the system robust and set the max displacement between every two epochs no exceed 20 meters.

The main differences between direct single point and IMU-assisted double difference model are as follows:

- Limited by smartphone clock oscillator quality, smartphone GNSS chips clock error drift dramatically affects system stability, PDD can eliminate the clock error of smartphone and satellite which reduce the system instability and the noise parameter estimator numbers.
- Double difference model sacrifices one equation in observation step where the max elevation angle satellite observation equation was set as the base reference.
- Double difference model is derived from single difference model which is derived from direct single point. Assuming the noise spectrum obeyed Gaussian distribution, difference process would generate double single difference noise variance. Theoretically, single point process noise is superposed into difference. Then PDD noise is combination of base-station noise and smartphone noise. For simplified calculation, the negligible base-station noise was ignored in this paper.
- Ionosphere and Troposphere were ignored in short base-line which is less than 10 km.

III. EXPERIMENT SETUP AND DATA PROCESSING

A. Setup

The experiment handheld platform was depicted in Fig 1. GNSS and ephemeris data were collected and processed by HUAWEI P10 which embedded a Broadcom BCM4774 chips. The GNSS antenna was installed in the upper of the phone, but the IMU model within P10 is unkown where the sampling rate of each inertial sensor was 50 Hz. A U-blox-m8n receiver with South HY-BLRB02R antenna was simultaneously experimented as a comparison. The ground truth was marked by U-blox-m8p RTK mode. At about 9.5 km distance from the experiment area, one CORS network is available. This station was used as base-station of our real-time difference system.

The experiments were carried out in the SJTU, Shanghai, China, with single point and IMU-assisted difference algorithm in different scenarios: static, kinematic, and signal blockage. The environment of experiments was shown in Fig 2.

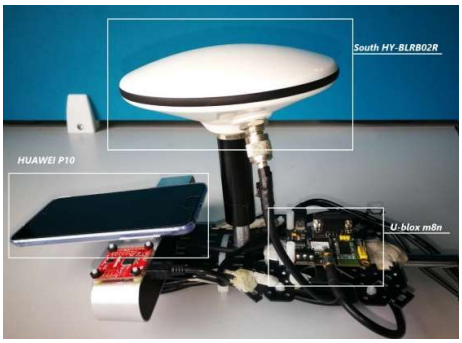

Fig. 1. The experiment handheld platform to collect data.

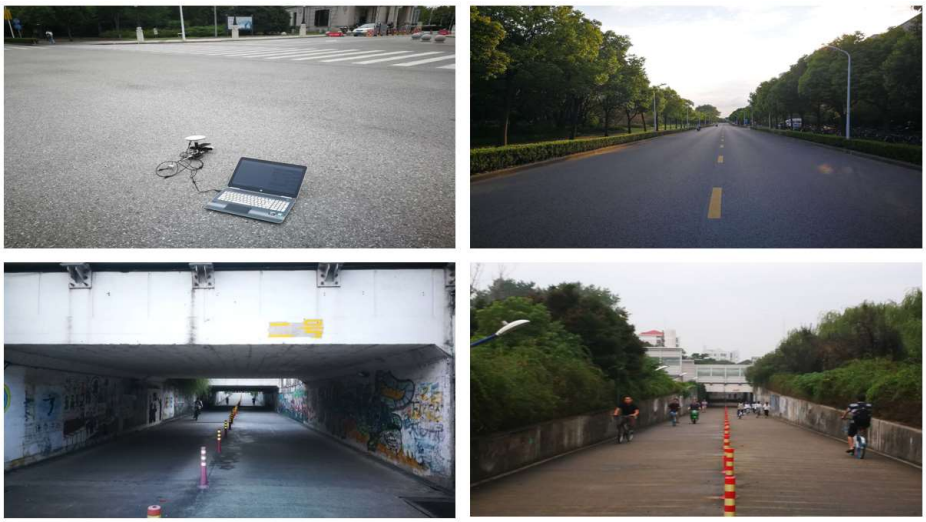
Fig. 2. The experiments were carried out in the campus of SJTU in different scenarios: static, kinematic, and signal blockage.

B. Data collection and processing

GNSS code measurements had been produced by GNSS chips in smartphone, but these available raw data should be transformed into Rinex format file by means of Android operating system API which were elaborately described by Android developer documents. The mainly adopted classes are ***GnssMeasurement*** and ***GnssClock***, which provided complete elements to generate Rinex format data such as pseudorange, carrier phase, Doppler and C/N0, detailed methods were introduced by [14]. The observables defined in Rinex format generation were depicted as Fig 3.

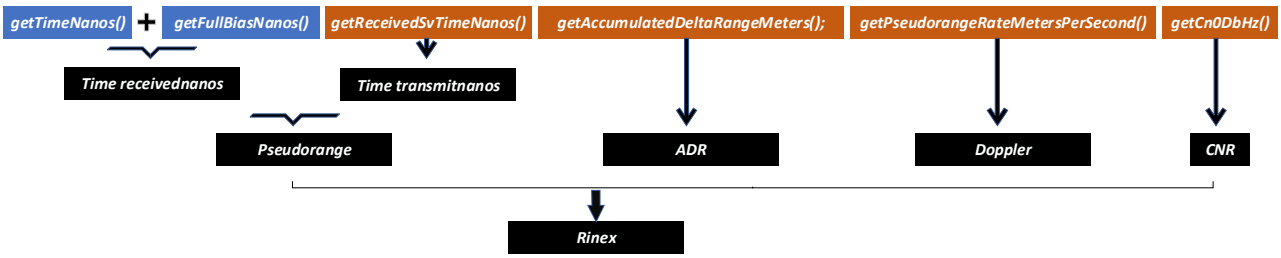

Fig. 3. Pseudorange generation, where blue blocks come from ***GnssClock*** and orange blocks come from ***GnssMeasurement***

It is worth noting that the method ***getFullBiasNanos*** gets the difference between clock inside GPS receiver and the true GPS time since January 6, 1980. This value is available if the receiver has estimated the GPS time which was acquired by local crystal. However, the crystal oscillator existed a fixed linear clock drift due to manufacturing technology, resulting in an increase in the

calculation of the bias (hundreds of nanoseconds per time) which presented in Fig 4. Before GPS positioning, it is better to lock the initial effective value of the ***FullBiasNanos***.

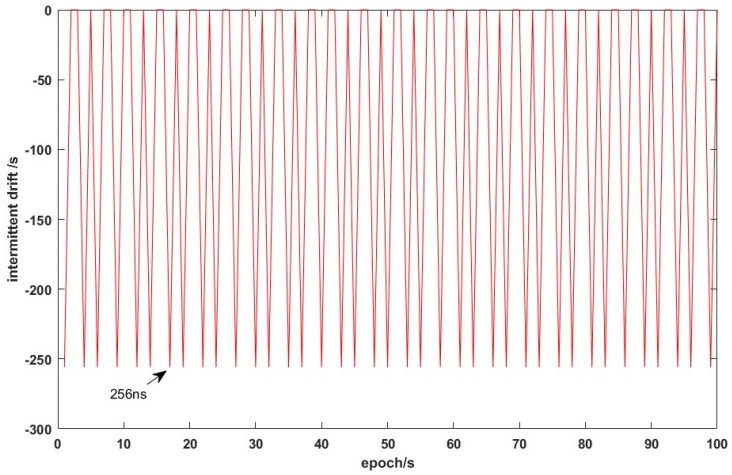

Fig. 4. The intermittent drift in smartphone GNSS clock

It is quite common knowledge that Android apps are written in Java. Java exists a drawback during the conversion between primitive type that it may generate a possible loss of precision. Float and double type are used to reduce storage space when storing rather than keeping high accuracy, frequent conversion data type operation may lead related time produce nanoscale bias which may lead several meters error in ultimate positioning result. Therefore, it is better avoiding to use float or double type to store data. Conversion between different orders of magnitude, such as the order of seconds and nanoseconds, should be as much as possible concentrated in one operation during calculation process.

API level 24 also provides some ***Uncertainty*** method to get the error estimate of GNSS data, in order to increase the data accuracy and reliability, we set up some threshold by experience：

1. ***getPseudorangeRateUncertaintyMetersPerSecond***() < 10m/s
2. ***getReceivedSvTimeUncertaintyNanos***() < 500ns
3. pseudorange value > 1e7 m & pseudorange < 3e7 m
4. Satellite angle > 15 degree & CNR > 15 dB
5. Max position movement per epoch < 10m

Inertial sensors measurements were usually used to assist navigation system. Android operating system offered several efficient sensor API to output optimized data. For example, the method ***getRotationMatrixFromVector*** is to get the rotation matrix ***R*** transforming a vector from the device coordinate system to which is defined as a direct orthonormal basis the ENU (East North up) coordinate system. ***SensorManager*** class also provides the sensor type: ***TYPE_LINEAR_ACCELERATION*** which can output a three dimensional vector indicating acceleration (no gravity) along each device axis.

The method ***registerListener*** registers a ***SensorEventListener*** for sensor at the given sampling frequency and the given maximum reporting latency. But the sampling frequency is only a hint to the system, events may be received faster or slower than the specified rate. Usually events are received faster, so the rotation matrix R and acceleration A are most likely not on the same frequency and a consistent rate method is essential.

Additional error sources affecting GNSS observations were also accounted for, such as relativistic effects caused by the Earth's rotation during signal propagation which would result a dekameter-lever effect and the satellite orbit eccentricity which results meter-level effect [2].

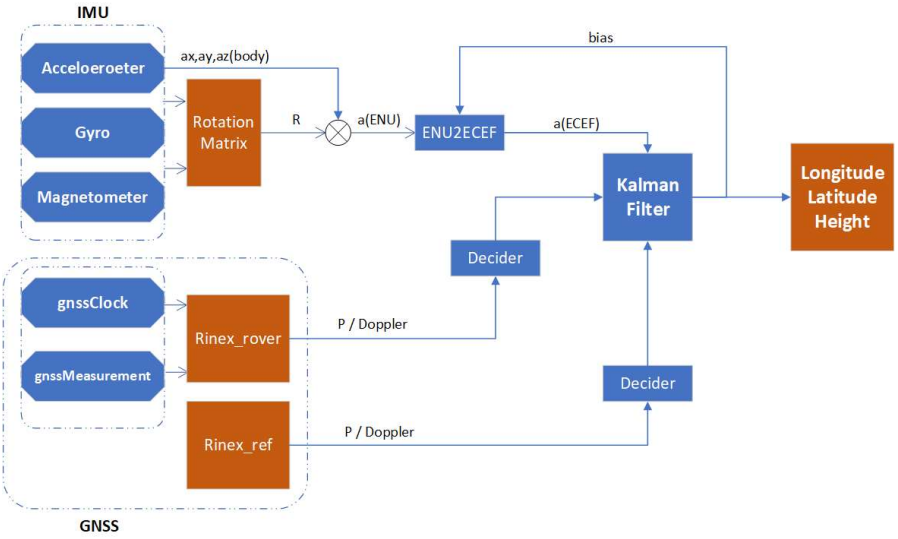

Fig. 5. PDD+IMU algorithm framework

Figure 5 shows the algorithm framework. All positioning processes were in the World Geodetic system 1984(WGS84) coordinate system. The real-time positioning results were converted into latitude and longitude, then mapped to Google Map.

IV. EXPERIMENT PERFORMANCE

The experimental results will be given below. Each positioning result would present a comparison of single point, PPD+IMU and U-blox-m8n, where ground truth was provided by U-blox-m8p RTK model.

Static：

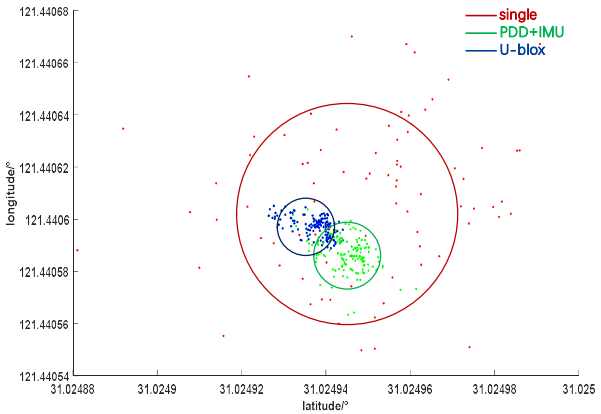

Fig. 6. The PDD+IMU static result

TABLE I
THE HORIZONTAL ERROR OF THREE METHOD IN STATIC SCENARIO

	Mean error (m)	Standard deviation (m)
Single point	4.51	9.57
PDD	4.11	3.99
U-blox-m8n	3.88	3.74

The static point test was set in the open area for 5 minutes and the well meteorological condition made the number of visible satellite signal was well enough. As the Fig 6 shows, the standard deviation of PDD is only 3.99 meters while single point error is 9.57 meters. 90% of the PDD position error is within 3.7 meters, which is close to U-blox-m8n. It denotes that the system uncertainty is acceptable.

Kinematic:

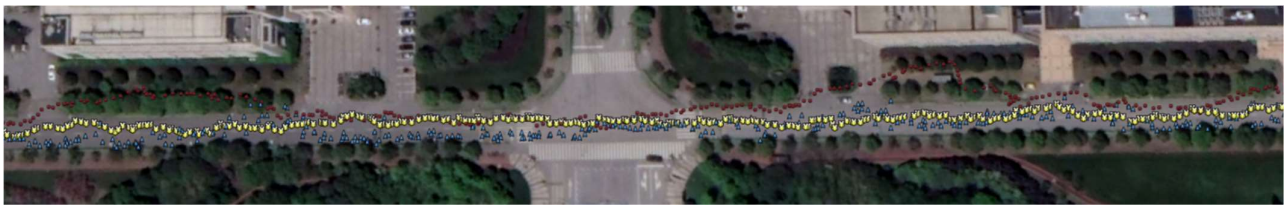

Fig. 7. The PDD+IMU kinematic result mapped in Google map.

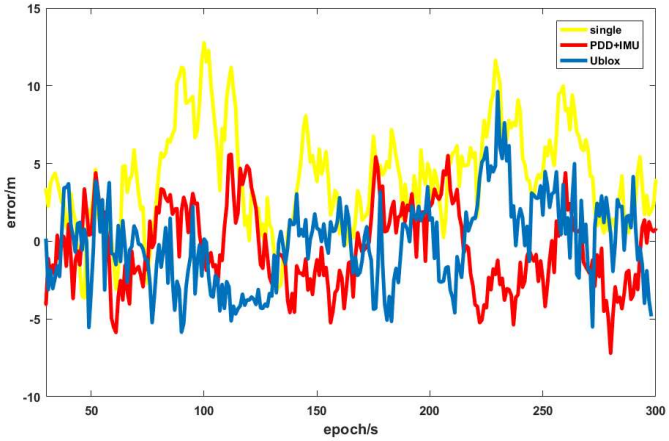

Fig. 8. The comparison curves of horizonal error.

TABLE II
THE HORIZONTAL ERROR OF THREE METHOD IN KINEMATIC SCENARIO

	Mean error (m)	Standard deviation (m)
Single point	6.77	5.00
PDD	3.71	2.60
U-blox-m8n	4.60	2.62

The kinematic test was executed for approximately 400s long the middle of the road where the trees on both sides are density but no buildings blocked the satellite signal. The comparison positioning results were presented as Fig 7. The errors of PDD assisted by IMU, PDD without IMU and direct single point are shown in Fig 8. The position curves proved that the PDD assisted by IMU performance exceeded two other model. The deviation is better than static test, an empirical explanation is that random antenna movement would reduce the multiple-path influence which made the curve converge well.

It is worthy to note that the middle of test route is an open area where no trees planted on either side. The mean error curve (about 150s-200s) and positioning result reflected on map also showed that this part apparently better than other part, which means the density trees had a bad effect on navigation signal. The best average solution was obtained by PPD with IMU assisted, the mean error and standard deviation also degraded than PDD without IMU. Comparing the two PDD test results in open road condition, IMU function of fusion sheme is slight, as Doppler is the dominant factor in determining the forward direction. The comparative experiment results show that IMU-assisted PDD algorithm can significantly improve the positioning accuracy, on open condition the mean error can be less than 4m and standard deviation can be less than 3m.

Blockage:

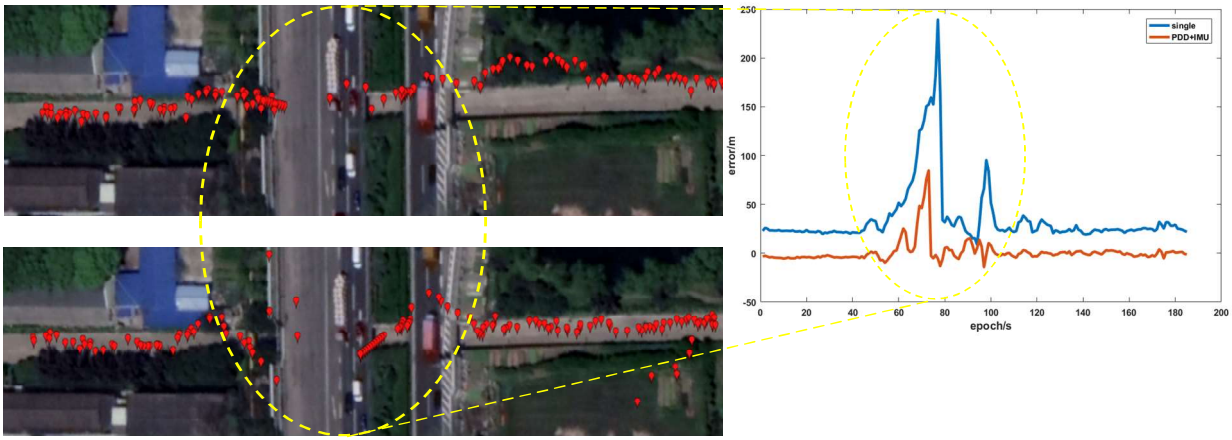

Fig. 9. The comparison results between PDD without IMU and PDD+IMU in tunnel

Another experiment was also carried out to test the robustness when the GNSS signal was blocked. The scenario was chosen in campus tunnel, where the road environment with 100 meters is worse than prior scene. In the middle of the road exist two short tunnels where the effective number of visible satellites was less than 4 and GNSS model could not independently afford right positioning information. On signal blockage condition, IMU provided all the motion information. As the result shows in Fig 9, the direct single point curve exists severe mutation curve, while PDD+IMU can slightly release the drastic drift and calibrate the fixed error. IMU effectively prevents large drifts in position but cannot be sufficient for long time reliability. Anyway, the result demonstrated that MEMS-based IMU enable to assist GNSS on smartphone.

V. CONCLUSION AND FUTRUE WORK

In this paper, we preliminary realize and verify the real-time high accuracy algorithm in the stand-alone smartphone platform using raw GNSS data. The algorithm of PDD assisted by IMU was established and the experiment architecture was introduced to present the details of data processing. During data collection we found smartphone clock error exists intermittent drift which can dramatically result a huge error of positioning. GNSS chips instability also lead the data obtained from Android is not ideal, extra thresholds are essential to filter it. The comparative results show that PDD assisted by IMU can effective increase the positioning accuracy and the real-time horizonal mean error enable to be 3.71 meters.

Future work will study the use of IMU to achieve better assistive techniques to help determine static motion state and more accurate motion trajectories in a short period of time.

.

ACKNOWLEDGMENTS

This work is supported by Shanghai Science and Technology Committee Research Project under Grant No.18DZ1100203 and National Natural Science Foundation of China under Grant No.61871265.

REFERENCES

[1] Azizyan M, Constandache I, Choudhury R R. SurroundSense:mobile phone localization via ambience fingerprinting[C]// DBLP, 2009:261-272. Banville S, Diggelen F V. Precise GNSS for Everyone: Precise Positioning Using Raw GPS Measurements from Android Smartphones[J]. Gps World, 2016, 27(11):43-48.

[2] Banville S, Diggelen F V. Innovation: Precise positioning using raw GPS measurements from Android smartphones. GPS World 2016, 11,7

[3] Pesyna K M J, Heath R W J, Humphreys T E. Centimeter positioning with a smartphone-Quality GNSS antenna[J]. 2014.

[4] Humphreys T E, Murrian M, Diggelen F V, et al. On the feasibility of cm-accurate positioning via a smartphone's antenna and GNSS chip[C]// Position, Location and Navigation Symposium. IEEE, 2016:232-242.

[5] Malkos, S. User Location Takes Center Stage in New Android OS: Google to Provide Raw GNSS Measurements. GPS World 2016, 27, 36.
[6] Kang W, Han Y. SmartPDR: Smartphone-Based Pedestrian Dead Reckoning for Indoor Localization[J]. IEEE Sensors Journal, 2015, 15(5):2906-2916.
[7] Gerdan G P. A comparison of four methods of weighting double difference pseudorange measurements[J]. Surveyor, 1995, 40(4):60-66.
[8] Takasu T, Yasuda A. Kalman-Filter-Based Integer Ambiguity Resolution Strategy for Long-Baseline RTK with Ionosphere and Troposphere Estimation[J]. Proceedings of International Technical Meeting of the Satellite Division of the Institute of Navigation, 2010, 7672(6):161-171.
[9] Tedaldi D, Pretto A, Menegatti E. A robust and easy to implement method for IMU calibration without external equipments[C]// IEEE International Conference on Robotics and Automation. IEEE, 2014:3042-3049.
[10] El-Sheimy N, Hou H, Niu X. Analysis and Modeling of Inertial Sensors Using Allan Variance[J]. IEEE Transactions on Instrumentation & Measurement, 2007, 57(1):140-149.
[11] F Wen, P Liu, H Wei, Y Zhang, RC Qiu, Joint Azimuth, Elevation, and Delay Estimation for 3-D Indoor Localization, IEEE Transactions on Vehicular Technology, 2018.
[12] W. Xie, F. Wen, J. Liu and Q. Wan, “Source Association, DOA, and Fading Coefficients Estimation for Multipath Signals,” IEEE Transactions on Signal Processing, vol. 65, no. 11, pp. 2773--2786, June 2017.